ANNALS OF GEOPHYSICS, 62, 1, VO13, 2019; doi: 10.4401/ag-8058

"PETROGRAPHIC AND SPECTROSCOPIC (FT-IR) STUDY OF WESTERN MEDITERRANEAN OBSIDIANS GEOLOGICAL SOURCES AND OF A LITHIC COLLECTION FROM USTICA ISLAND (SICILY)"

Mariangela La Monica[1], Silvio Giuseppe Rotolo[1,3], Franco Foresta Martin[*,2,3]

(1) Università di Palermo, Dipartimento di Scienze della Terra e del Mare (DiSTeM), Palermo, Italy
(2) Laboratorio Museo di Scienze della Terra Isola di Ustica, Palermo, Italy
(3) Istituto Nazionale di Geofisica e Vulcanologia, Sezione di Palermo, Italy

Article history
Receveid **December 12, 2018**; accepted **January 28, 2019**.
Subject classification:
Obsidian, Petrographic study, FT-IR, Mediterranean obsidians, Ustica Island.

ABSTRACT

In this study we applied petrochemical methods (SEM-EDS; FT-IR) in order to characterize a group of obsidian flakes collected at Ustica island (Sicily). Despite the absence of obsidian geological outcrops, a lot of obsidian fragments still emerging from the lands of Ustica testify that the island was a major import center of obsidian during the prehistory. On this island, there are some prehistoric settlements, dated from the Neolithic to the Middle Bronze Age (6000- 1200 BC), in which the use of obsidian continued until the beginning of metals age. Our study includes: i) Macroscopic and microscopic optical observations, which allowed selecting 18 obsidian flakes (starting from 50 obsidian flakes) on the base of their morphological characteristics. ii) Density measurements (hydrostatic balance). iii) Scanning electron microscope determination (SEM-EDS) of major elements of the obsidian glasses and minerals.

Results of our analyses were compared with 12 geological samples collected in obsidian sources from Monte Arci (Sardinia), Palmarola, Lipari and Pantelleria, i.e. the four most exploited obsidian sources of the ancient world in the Western-Central Mediterranean. This study confirms the presence of the Lipari and Pantelleria sources (Sicily) in our obsidian set. iv) We also determined (by FT-IR) the hydration degree of some obsidian flakes in order to detect a possible hydration gradient between the rim and the core of the flake sample. The width of the hydration rim, if any, can be used for an approximate evaluation of the age of the tool.

1. INTRODUCTION

Obsidians are volcanic glass, generally black to grey or green in color, originated by rapid cooling of viscous lava, a process that inhibits or minimizes crystal growth. Their silica content is high (SiO_2 = 65% to 80%, trachytic to rhyolitic compositions), and commonly H_2O poor (< 1.0 %). During the prehistory obsidian chunks were transferred from geological outcrops to distant human settlements, and due to their workability they were widely used to create cutting tools and weapons [Williams-Thorpe, 1995].

In this work, 18 obsidian fragments out of a total of 50, were recovered in the proximity of Ustica's prehistoric settlements and were then analyzed for their petrochemical characterization (SEM-EDS), in comparison with obsidians directly sampled in the four major outcrops of western Mediterranean exploited during the prehistory.

SEM-EDS analysis of the major elements has been performed both on the vitreous mass of each obsidian sample and on the microphenocrysts present in it, i.e.: pyroxenes, biotites, feldspar, etc. As some authors have shown, the integration of all these analytical data offers more reliable criteria for characterizing the original sources [Acquafredda and Paglionico, 2004].

Obviously, the SEM-EDS analysis of the vitreous mass and of microphenocrysts requires the preparation of thin section obtained from a small fragment of the sample, and therefore it must be considered a partially destructive process, not applicable in the case of obsidians with archaeological significance.

Besides tracking back obsidian tool fragments to their original sources, in this paper we present also results of a Fourier Trasformate-Infrared Spectroscopy (FT-IR) study on the hydration of edges of obsidian cutting tools. The width of hydration halo is in fact a function of the time elapsed since the cutting and shaping of the tool from the original obsidian raw block [Skinner, 1995].

2. THE EXTRACTIVE AREAS OF THE OBSIDIAN IN THE PERI-TYRRHENIAN ZONE

In the peri-Tyrrhenian area, there are four main geological sources of obsidian, all located in Italian islands: (i) *M. Arci* (Sardinia), (ii) *Palmarola* (Pontine Islands), (iii) *Lipari* and (iv) *Pantelleria* (Sicily) (Figure 1). These four obsidian sources fed the obsidian commerce in Western and Central Mediterranean, from Neolithic to Bronze Age (6000- 1200 BC) [Williams - Thorpe, 1995; Acquafredda et al., 1999; Acquafredda and Paglionico, 2004; Bigazzi et al., 2005]. Here follows a brief summary of the geological outlines of these obsidian sources.

2.1 MONTE ARCI

Monte Arci is located in the western side of Sardinia (Campidano region) and its volcanism spanned through Tertiary to Quaternary. The Monte Arci complex lies along the north-eastern border of the Campidano Graben. The volcanic activity was characterized by four distinct eruptive episodes, with quite different erupted magmas: phase 1, rhyolites; phase 2, dacites and andesites; phase 3, quartz-normative trachytes; phase 4, mafic lavas ranging from subalkaline to mildly alkaline. The first phase was the one that generated metaluminous rhyolites with obsidians enclaves [Montanini, 1992; Montanini et al., 1994]. Many age determinations on M. Arci obsidians have been performed by various authors: the most recent, with the $^{40}Ar/^{39}Ar$ method, indicate an age of about 3,5 Ma [Bellot-Gurlet et al., 1999], in good agreement with the measures previously carried out by Montanini and Villa [1993].

From a minimum of 3 to 7 chemically different subsources of obsidians have been recognized by various authors throughout the Monte Arci complex; but for archaeological purposes only 4 subsources are currently indicated, conventionally defined with the following abbreviations: SA, SB1, SB2 and SC [Williams-Thorpe et al., 1984; Tykot, 1996; De Francesco and Crisci, 1999, 2003; De Francesco et al., 2004].

The obsidian of Monte Arci are generally opaque, grayish in color and are rich in biotite phenocrysts (up to 300 microns) visible to the naked eye.

2.2 PALMAROLA

The Island of Palmarola is located in the Pontine Archipelago, in the Central-eastern Tyrrhenian Sea. The volcanic activity of Palmarola, related to the spreading of the Tyrrhenian Sea, began in the Upper Pliocene and Pleistocene [De Rita et al., 1989]. The most important obsidian deposit (for volume and quality) is Monte Tramontana and it is located in the northern part of Palmarola [Tykot et al., 2005].

The age of Monte Tramontana obsidians is 1.7 Ma, according to analysis carried out with the fission track method by Bigazzi et al. [1971]. This result is in agreement with that obtained by Barberi et al. [1967] on the rhyolitic lava domes of the island. More recent measures by Bellot-Gurlet et al. [1999] differ a little from previous values.

The obsidians of Palmarola exhibit black to greyish color and can be opaque or shiny; transparent when observed in thin flakes and microphenocrysts poor.

2.3 LIPARI

Lipari Island is located in the Aeolian Archipelago (Sicily). The volcanic history of the island has been subdivided into nine different Eruptive Epochs, from about 267 ka to the medieval period. Magmas erupted during the first six periods were mafic to intermediate to felsic (basaltic andesites, andesites to rhyolites). Rhyolitic obsidians were emplaced only during the last 43 ka [Forni et al., 2013].

According to literature, only two obsidian outcrops of Lipari were exploited during prehistoric times: Vallone del Gabellotto and Canneto Dentro [Tykot, 1996; Bigazzi et al., 2005]. Vallone del Gabellotto, which was the most exploited outcrop during prehistory for the high quality of glass, has an age of 8.7-8.4 ka [Zanchetta et al., 2011]. Canneto Dentro obsidian is

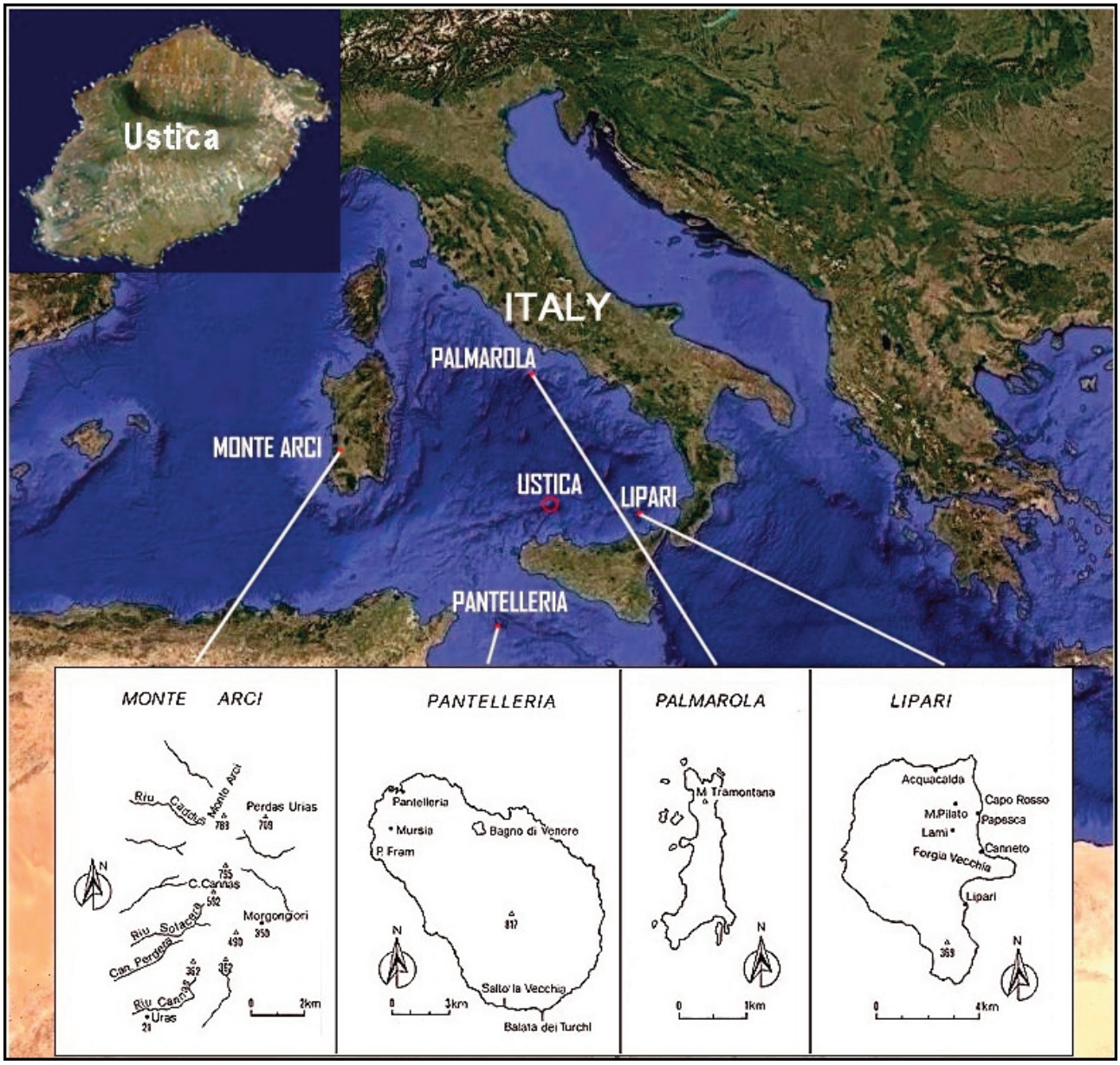

FIGURE 1. The four obsidian sources of the peri-Tyrrhenian area exploited during the prehistory: *M. Arci* (Sardinia), *Palmarola* (Pontine Island), *Lipari* and *Pantelleria* (Sicily); and the island of Ustica where the archaeological obsidians analyzed in this work were found. Modified after Acquafredda et al., 2004, and after Google Earth.

older, about 20 ka, and was utilized far less frequently [Forni et al., 2013; Freund, 2017].

Many others important obsidian deposits are concentrated in the north-eastern part of the island at Punta di Sparanello, Forgia Vecchia and Rocche Rosse, but their formation dates back to historic times and consequently could not have been exploited by Stone Age civilizations.

The obsidians of Lipari are black or greyish colored, transparent on the thin edges, and contain quartz and feldspars microphenocrysts; sometimes are variably devitrified (spherulite-bearing).

2.4 PANTELLERIA

Pantelleria is a volcanic island located in the Sicily Channel, between Sicily and Tunisia. Pantelleria is the type-locality of pantellerite rocks, peralkaline rhyolites enriched in Na, Fe, Cl, and incompatible trace elements, especially Zr and Nb [Civetta et al., 1988]. The island is composed chiefly of pantelleritic tephra (pumice falls and ignimbrites) and lavas. The three know obsidian sources belonging to rather old lava flows (age 250-190 ka) are: *Balata dei Turchi*, *Salto La Vecchia*, and *Lago di Venere* [Acquafredda and Paglionico, 2004].

Pantelleria obsidians exhibit a greenish colour when

thin flakes are observed under transmitted light [Francaviglia, 1984]: thanks to this macroscopic distinctive characteristic it is possible to distinguish them from the others peri-Tyrrhenian obsidian sources.

3. THE ISLAND OF USTICA

Ustica is a volcanic island, located in the southern Tyrrhenian Sea, (Figure 1), with a maximum elevation of 248 m at Monte Guardia dei Turchi. It represents the emerging top of a vast submerged volcanic complex rising more than 2000 m from the bottom of the sea [de Vita et al., 1995].

Ustica volcanic history begun with submarine eruptions that formed pillow lavas and hyaloclastites. After the emersion of the island, subaerial activity alternated emission of basaltic lava flows and explosive eruptions (hydromagmatic to subplinian to strombolian). Erupted magmas are for the vast majority alkali basalts, but a small volume of felsic (trachytic) tephra also occur [de Vita, 1995; de Vita et al., 1998]. Present-day landscapes are the result of the complex interplay between glacio-eustatic sea-level oscillations, which produced 5 orders of marine terraces, gravitative collapses, and faults. Marine terraces created flat surfaces that constituted the site of the most important archaeological settlements, where a great number of obsidian artifacts were found. It must be noted that there are not obsidian rocks in the geological record of Ustica, therefore, all the obsidian flakes recovered on the land are allochthonous, and they are the result of exchanges and trades made during prehistory [Foresta Martin et al., 2017; Foresta Martin and La Monica, 2018].

4. SAMPLING

We examined a group of 10 geological samples collected in situ by the authors in geological obsidian sources: (i) *Pantelleria* (1 sample from *Salto la Vecchia*), (ii) *Sardinia* (3 samples from western side of *Monte Arci*, near *Marrubiu*), (iii) *Lipari* (3 samples from *Pomiciazzo*, *Forgia Vecchia*, *Rocche Rosse*), (iv) *Palmarola* (3 samples from La Radica- Central-east coast). We also examined 18 archaeological samples (Figure 2) collected on the surface of the island of Ustica. These samples belong to the 'Museo della Parrocchia di San Ferdinando Re' of Ustica and were collected by the late C. G. Seminara, honorary inspector of the 'Soprintendenza BB.AA.CC'. of Palermo, in the surroundings of the main archaeological settlements of the island. Unfortunately, we do not have any specific information about the sampling location, but we know that this collection spans a time interval ranging from the Neolithic to the Bronze Age [Foresta Martin et al., 2016].

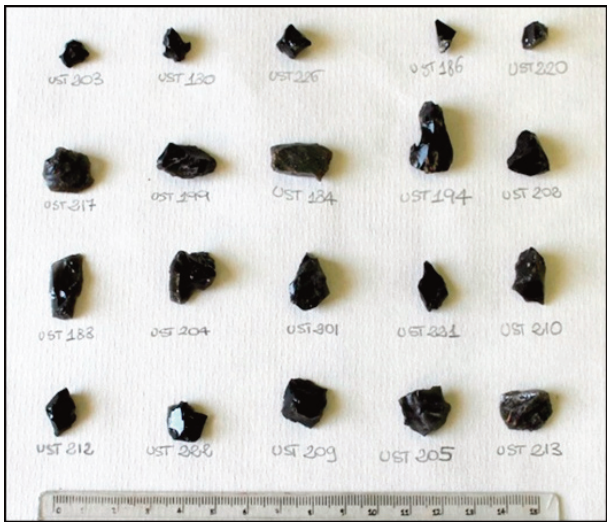

FIGURE 2. Obsidian flakes collected at Ustica.

Samples were analysed at the laboratories of the Dipartimento di Scienze della Terra e del Mare (DiSTeM- Università di Palermo) and at the laboratories of the INGV-Istituto Nazionale di Geofisica e Vulcanologia in Palermo.

5. ANALYTICAL METHODS

The characterization of the physical and chemical properties of the geological and archaeological obsidian was carried out through:

i) Visual observations with naked eye and with optical microscope, in order to define some primary diagnostic features such as color, banding, luster, inclusions, and crystallinity. Microscopic observations were carried out on thin sections 50 to 150 microns thick;

ii) Density measurements with a high-precision analytical balance, equipped with a device for immersion of the sample in distilled water (after ultrasonic cleaning). Measurements were done at the 4th decimal digit. Samples were treated in order to remove any adhering air bubbles and the water temperature was carefully measured with a mercury thermometer;

Geological samples	Locality	Color*	Color**	Luster	Microlites	Phenocrysts
PANT-1	Pantelleria S.L.V	black	green	opaque	yes	no
PANT-2	Pantelleria	black	green	opaque	yes	no
PANT-3	Pantelleria	black	gray- green	opaque	yes	no
PALM-1	Palmarola	black	brown	shiny	no	no
PALM-2	Palmarola	dark-gray	brown	opaque	no	no
PALM-3	Palmarola	black	brown	vitreous -shining	no	no
M.ARCI-1	Sardegna	dark gray	dark - gray	vitreous -shining	yes	yes
M.ARCI-2	Sardegna	black	dark - gray	vitreous -shining	yes	yes
M.ARCI-3	Sardegna	black	dark - gray	vitreous -shining	yes	yes
LIPARI-1	Lipari-Pom.	dark gray	light- gray	vitreous	no	no
LIPARI-2	Lipari F.Ve.	light gray	light- gray	vitreous	no	no
LIPARI-3	Lipari-R.R.	black (devretification)	gray	vitreous	no	no

TABLE 1. Main macroscopic and microscopic characteristics of geological samples. Phenocrysts = (ϕ >100 μm); Microlites = (ϕ < 50 μm). S.L.V. = Salto la Vecchia; Pom = Pomiciazzo; F.Ve= Forgia Vecchia; R.R. = Rocche Rosse. * naked eye. ** optical microscope.

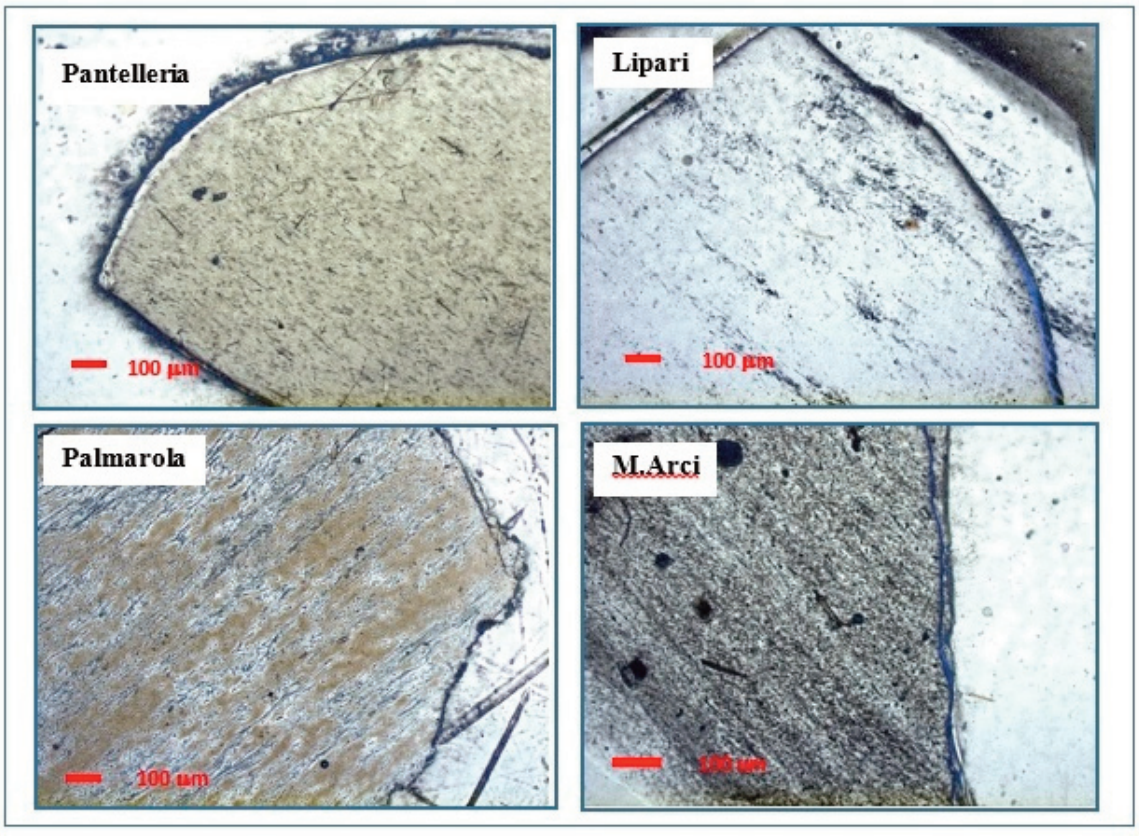

FIGURE 3. Microphotos of the obsidian geological samples from Pantelleria, Lipari, Palmarola and Monte Arci (optical microscope, Magnification 10 X).

Archaeological samples	Locality	Color*	Color**	Luster	Microlites	Phenocrysts
UST-180	Ustica	black- green	green	opaque	yes	no
UST-186	Ustica	black	gray	opaque	no	no
UST-191	Ustica	black (devetrification)	colourless	transparent	yes	no
UST-192	Ustica	gray	colourless	transparent	no	no
UST-195	Ustica	black	green	opaque	yes	no
UST-201	Ustica	dark gray	colourless	transparent	yes	no
UST-203	Ustica	black- green (banding)	light- green	opaque	yes	no
UST-206	Ustica	black	colourless	transparent	no	no
UST-208	Ustica	dark gray (devetrification)	light- gray	transparent	no	no
UST-211	Ustica	dark gray (devetrification)	colourless	transparent	yes	no
UST-212	Ustica	black- green	gray	opaque	yes	no
UST-215	Ustica	black	gray	transparent	no	no
UST-220	Ustica	dark gray	gray	transparent	no	no
UST-221	Ustica	black	gray			
(banding)	opaque	no	no			
UST-222	Ustica	black	colourless	transparent	no	no
UST-223	Ustica	green				
(banding)	green (banding)	opaque	no	no		
UST-224	Ustica	black	colourless	transparent	yes	no
UST-226	Ustica	black	colourless	transparent	yes	no

TABLE 2. Principal macro- and microscopic features of archaeological samples. Phenocrysts = (ϕ >100 $\mu\mu$m); Microlites = (ϕ < 50 μm). * naked eye. ** optical microscope

iii) Scanning electron microscope (SEM-EDS) for textural observations and microanalysis of minerals and glasses. Mineral and glass analysis were performed on polished samples mounted in epoxy, using a LEO™ 440 scanning electron microscope coupled to an Oxford-Link EDS. Operating conditions were: 20 kV accelerating voltage and 600 pA beam current. Natural mineral stan-

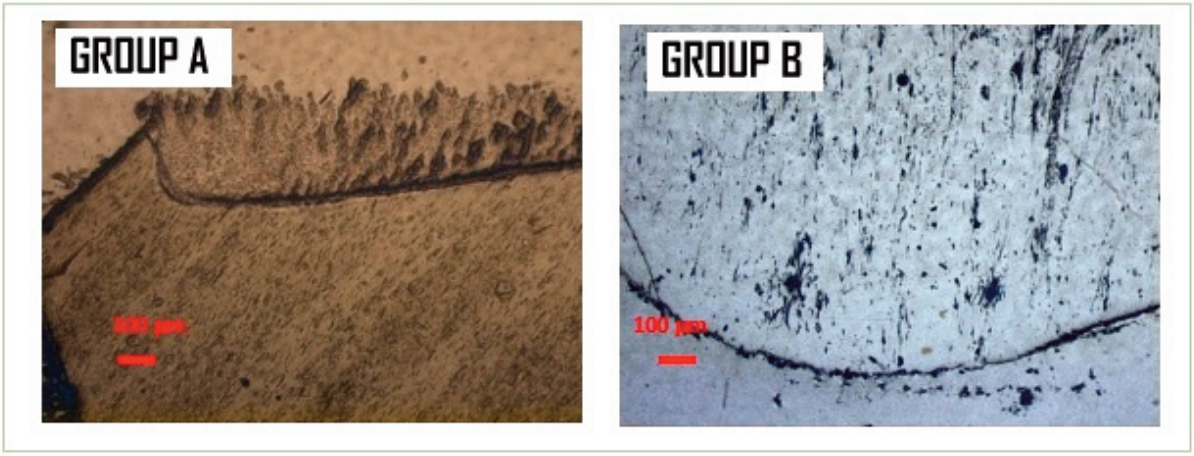

FIGURE 4. Microphotos of the archaeological (optical microscope, 10x). Group A: greenish obsidians; Group B: greyish obsidians.

dards were used to calibrate quantitative analysis; iv) determination of H_2O content by Fourier-Transform Infrared Spectroscopy (FT-IR). The determination of water content was carried out at DiSTeM, using a Bruker Hyperion 2000 FT-IR spectrometer coupled with a microscope (fluxed with CO_2-and H_2O-free compressed air). Doubly polished obsidian flakes (60-100 µm thick) were mounted on a ZnSe disk for FT-IR analysis. Sample spectra and background were acquired in the 1000-6000 cm^{-1} absorption range with a resolution of 2 cm^{-1}, adopting a Globar source with a MCT detector and scan rate of 20 kHz and completing 256 scans. We performed also the determination of water content by (FT-IR) spectroscopy on selected obsidian flakes where the original cut made by the toolmaker was clearly identified, spotting analytical points from rim to core, along a transect normal to flake edge. This procedure allows detecting a possible hydration gradient and making a rough evaluation of the age since the time of obsidian chipping, according to a method developed for the first time by Friedman e Smith [1960] and later improved by other authors [i.e. Skinner, 1995; Stevenson et al., 2002; Liritzis and Laskaris, 2011].

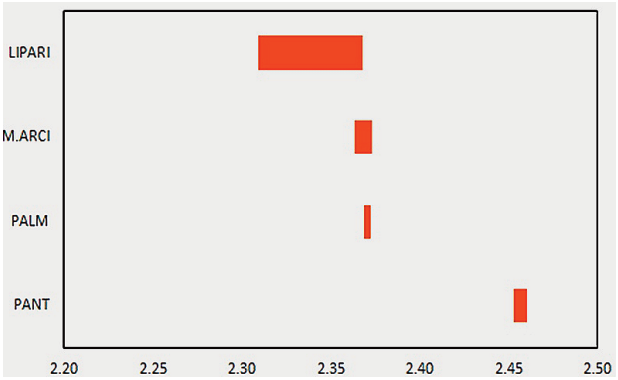

FIGURE 5. Density (g cm^{-3}) of obsidian samples from Lipari, M. Arci, Palmarola (Palm) and Pantelleria (Pant).

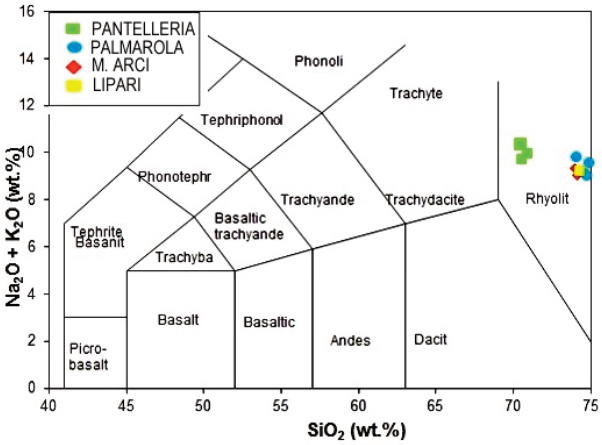

FIGURE 6. Total alkali vs silica diagram (le Bas et al., 1986) of the geological samples. All samples plot in the field of rhyolites. Pantelleria (green), Palmarola (blue), Monte Arci (red), Lipari (yellow).

6. RESULTS

We present here analytical data on a group of 10 geological and 18 archaeological obsidian samples in order to characterize their physical and petrochemical properties, with the aim to trace back archaeological samples to their possible geological sources.

6.1 VISUAL OBSERVATIONS

Naked eye visual observations of the geological obsidians allowed describing the main physical external

Geological samples	Palm1		Palm2		Palm3		M.Arci1		M.Arci2		M.Arci3		Lipari-1		Lipari-2		Lipari-3		Pant-0653
Site	Radica		Radica		Radica		Marrubbiu		Marrubbiu		Marrubbiu		Pomiciazzo		Forgia Vecc.		Rocche Rosse		Salto la Vecchia
Density * g/cm^3	2.3683		2.3700		2.3723		2.3733		2.3646		2.3631		2.3554		2.2968		2.3090		
Density ** g/cm^3	2.3525		2.3524		2.3532		2.3427		2.3538		2.3534		2.3570		2.3570		2.3526		
SiO_2	74.60	0.38	74.77	0.49	74.66	0.57	74.93	0.08	74.11	0.33	73.94	0.15	74.33	0.22	74.27	0.03	74.13	0.29	72.71
TiO_2	0.19	0.06	0.12	0.10	0.01	0.01	0.12	0.00	0.23	0.11	0.15	0.12	0.00	0.09	0.08	0.13	0.07	0.15	0.23
A_2O_3	14.09	0.18	14.21	0.30	14.10	0.19	14.34	0.16	14.60	0.14	14.63	0.05	14.04	0.26	13.91	0.16	13.72	0.11	6.49
FeO	1.45	0.13	1.47	0.13	1.59	0.14	0.61	0.04	1.12	0.16	1.14	0.03	1.71	0.09	1.65	0.03	1.48	0.12	9.38
MnO	0.00	0	0.02	0.04	0.13	0.02	0.00	0.00	0.09	0.08	0.10	0.05	0.15	0.00	0.05	0.04	0.14	0.00	0.29
MgO	0.00	0	0.0	0	0.01	0.05	0.00	0.07	0.08	0.12	0.06	0.11	0.00	0.11	0.06	0.07	0.00	0.09	0.00
CaO	0.45	0.09	0.44	0.10	0.48	0.07	0.76	0.12	0.78	0.09	0.80	0.03	0.80	0.17	0.80	0.10	0.77	0.02	0.28
Na_2O	3.75	0.21	3.53	0.26	3.70	0.40	3.16	0.04	3.05	0.10	3.17	0.18	3.50	0.09	3.37	0.20	3.58	0.15	7.23
K_2O	5.49	0.22	5.47	0.12	5.38	0.13	6.35	0.05	5.99	0.09	6.15	0.12	5.71	0.16	5.67	0.08	6.20	0.08	3.34
P_2O_5	0.00	0	0.01	0.01	0.00	0	0.00	0.00	0.00	0	0.00	0.00	0.00	0.00	0.00	0.00	0.00	0.00	0.00
P.I.	0.86	0.03	0.83	0.004	0.85	0.06	0.84	0.02	0.79	0.01	0.81	0.03	0.85	0.02	0.84	0.03	0.92	0.02	2.39
Na_2O/K_2O	0.68	0.05	0.65	0.04	0.69	0.07	0.5	0.002	0.51	0.02	0.52	0.03	0.61	0.03	0.60	0.04	0.58	0.03	2.16

TABLE 3. Major elements determined by SEM-EDS analyses (using a defocused beam) on samples of the four peri-Tyrrhenian obsidians. P.I. (peralkalinity Index) = Na_2O+K_2O/Al_2O_2 . N= number of glass analyses* Density measurements using an analytical balance (mean of 3 measurements). ** Density calculated according to Ochs e Lange (1999).

Archaeological samples	Locality	Color*	Color**	Luster	Microlites	Phenocrysts
UST-180	Ustica	black- green	green	opaque	yes	no
UST-186	Ustica	black	gray	opaque	no	no
UST-191	Ustica	black (devetrification)	colourless	transparent	yes	no
UST-192	Ustica	gray	colourless	transparent	no	no
UST-195	Ustica	black	green	opaque	yes	no
UST-201	Ustica	dark gray	colourless	transparent	yes	no
UST-203	Ustica	black- green (banding)	light- green	opaque	yes	no
UST-206	Ustica	black	colourless	transparent	no	no
UST-208	Ustica	dark gray (devetrification)	light- gray	transparent	no	no
UST-211	Ustica	dark gray (devetrification)	colourless	transparent	yes	no
UST-212	Ustica	black- green	gray	opaque	yes	no
UST-215	Ustica	black	gray	transparent	no	no
UST-220	Ustica	dark gray	gray	transparent	no	no
UST-221	Ustica	black	gray			
(banding)	opaque	no	no			
UST-222	Ustica	black	colourless	transparent	no	no
UST-223	Ustica	green				
(banding)	green (banding)	opaque	no	no		
UST-224	Ustica	black	colourless	transparent	yes	no
UST-226	Ustica	black	colourless	transparent	yes	no

TABLE 3. Continued.

Site Geological samples	Palmarola Palm2	Palmarola Palm2	Palmarola Palm2	Lipari Lip2	Lipari Lip3
SiO_2	51.00	49.44	49.80	48.37	49.56
TiO_2	0.26	0.59	0.25	0.17	0.08
Al_2O_3	2.44	2.20	0.75	0.84	2.88
FeO	24.90	24.68	25.31	28.88	25.44
MnO	2.59	2.52	2.64	3.11	1.31
MgO	3.78	3.93	4.75	2.21	1.11
CaO	13.62	15.68	15.74	16.48	18.41
Na_2O	0.86	0.97	0.72	0.20	0.94
K_2O	0.38	0.15	0.15	0.06	0.05
Tot.	99.84	100.16	100.11	100.32	99.79
Wo%	35.55	38.81	37.38	39.15	46.24
En%	13.74	13.53	15.71	7.30	3.89
Fs%	50.71	47.66	46.91	53.55	49.86
Mg/Mg+Fe * 100	21.31	22.11	25.09	12.00	7.24

TABLE 4. Major elements analyses (determined by SEM-EDS) of clinopyroxene microphenocrysts on geological samples from Lipari and Palmarola.

features such as color, luster and presence of phenocrysts. Microscopic observations were carried out with an optical microscope (10x) on obsidian wafers 50 to 150 microns thick, establishing relevant optical differences among the four geological sources.

Here we list the main distinctive features that we have highlighted in the analysed geological samples (Table 1; Figure 3).

- Pantelleria obsidian (1 sample) is greenish in color with tiny microphenocrysts of alkali feldspar scattered in the glassy matrix;
- Lipari obsidians (3 samples) are greyish in color with tiny microphenocrysts of alkali feldspar and clinopyroxene scattered in the glassy matrix;
- Palmarola obsidians (3 samples) are instead characterized by a brown banding (8-10 mm thick) at any depth of the sample, and the color is greyish;
- Monte Arci obsidians (3 samples) are instead greyish in color but their most peculiar pattern is the occurrence of biotite microphenocrysts up to 150 μm in length.

Microscopic observations of the archaeological samples (Table 2; Figure 4) were carried out on obsidian wafers 50 to 150 microns thick, which allowed differentiating two main groups:

- Group A, consisting of 5 out of 18 samples (27%) includes obsidians greenish in colour and with many feldspars and subordinate clinopyroxene microphenocrysts;
- Group B, consisting of 13 out of 18 samples (73%) all greyish in colour with many clinopyroxene microphenocrysts.

6.2 DENSITY MEASUREMENTS

Density measurements show that Group A samples range between 2,45 - 2.47 g cm-3 in clear overlap with the typical density of Pantelleria peralkaline rhyolites (i.e. pantellerites). The Group B density cluster is in the range 2,35- 2.37 g cm-3, namely an interval typical of obsidians of Lipari, Palmarola and Monte Arci as well. Results of density measurements are summarized in the Table 3 and Figure 5.

In order to verify the accuracy of the experimentally measured densities, these latter were compared with the densities calculated according to Ochs and Lange [1999], taking into account the average glass

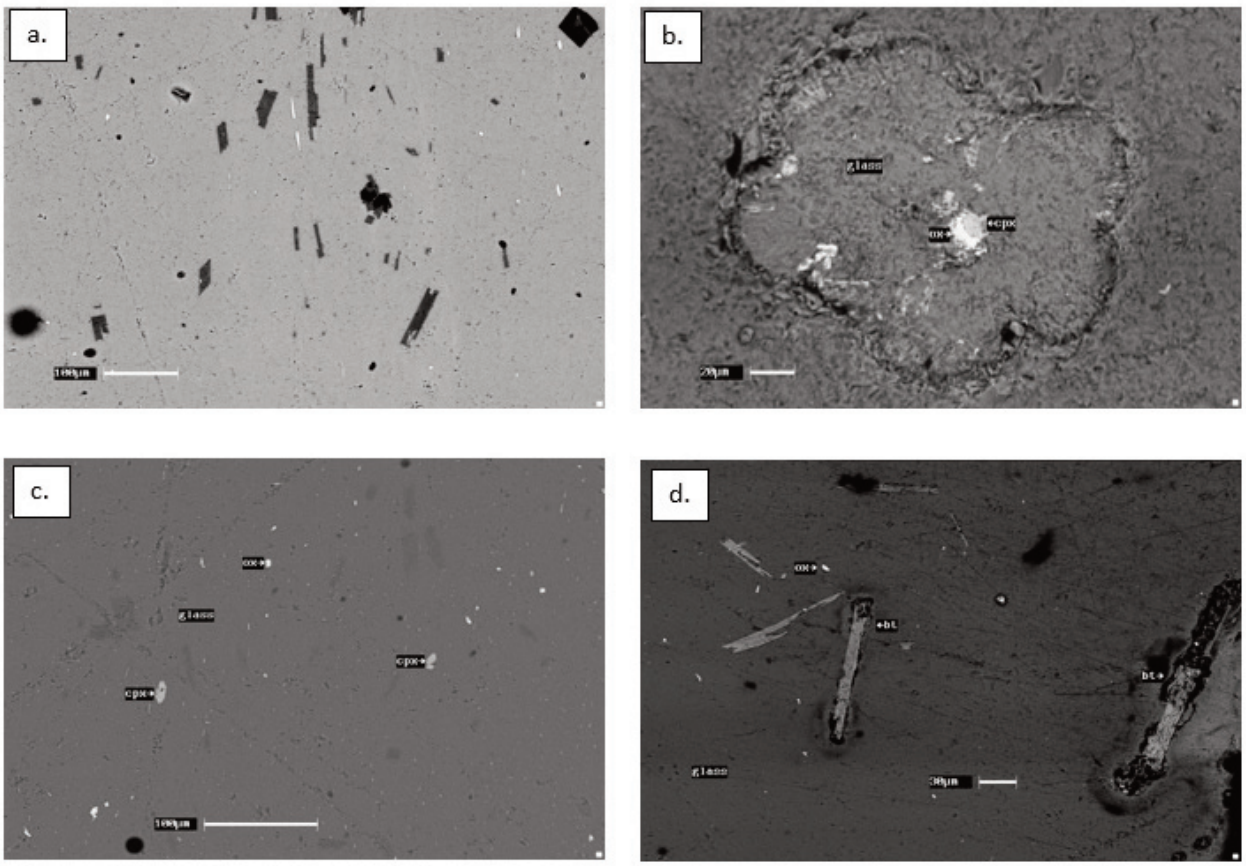

FIGURE 7. SEM-BSE images of polished thin sections of geological samples. a) Pantelleria obsidian (Salto La Vecchia). Sparse Feldspar microlites are set in a glassy matrix. b) Lipari obsidian : rare clinopyroxene microphenocrysts (30-40 μm in size, subhedral to anhedral) set in a slightly devitrified matrix; c) Palmarola. clinopyroxene microlites (~40 μm in size); d) section of Monte Arci - microphenocrysts of biotite (gray) are clearly distinguishable.

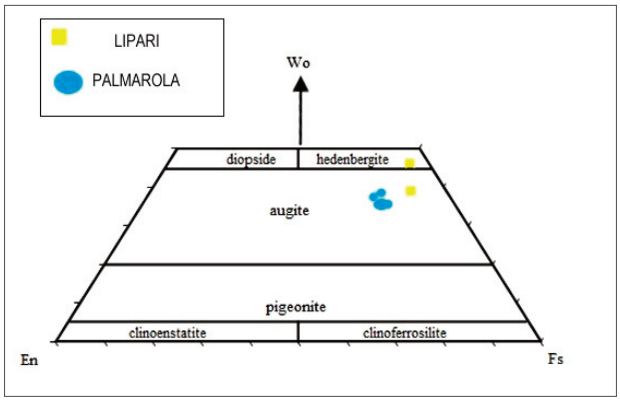

FIGURE 8. Composition of pyroxenes of the geological samples according to the nomenclature by Morimoto et al. [1989]. Lipari clynopyroxenes (yellow square) ranging from augite to hedenbergite, Palmarola clynopyroxenes (blue circle) are augite.

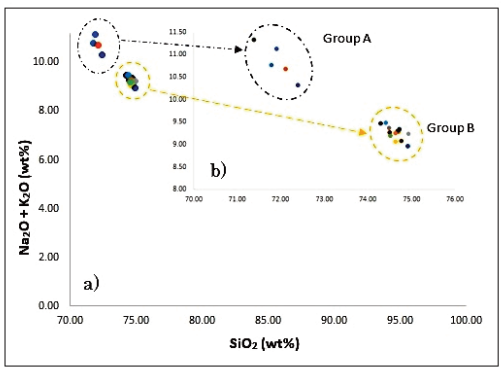

FIGURE 9. TAS diagram of archaeological samples. All samples plot in the field of rhyolites. Group A samples (circle blue) have P.I. >1; Group B samples (circle yellow) have P.I. < 1.

chemical analysis. It was possible to ascertain that the difference between experimental and calculated density does not exceed the second decimal digit. Further on, we will report the results of these compared measures.

6.3 PETROCHEMISTRY OF GEOLOGICAL SAMPLES

Results of microanalyses (SEM-EDS) of major elements related to the geological obsidian samples are summarized in the Table 3. Whereas in Table 4 are reported SEM-EDS analyses of major elements related to clinopyroxene microphenocrysts present in the obsidian samples.

Archaeological samples	Ust180		Ust186		Ust191		Ust192		Ust195		Ust201		Ust203		Ust206		Ust208	
Site	Pantelleria		Pantelleria		Lipari		Lipari		Pantelleria		Lipari		Lipari		Lipari		Lipari	
Density * g/cm^3	2.4719		2.4483		2.3494		2.3377		2.4697		2.3440		2.3323		2.3466		2.3559	
Density ** g/cm^3	2.4253		2.4229		2.3372		2.3512		2.4220		2.3507		2.3556		2.3515		2.3536	
N	4	St.d 2σ	3	St.d 2σ	3	St.d 2σ	4	St.d 2σ	3	St.d 2σ	4	St.d 2σ	3	St.d 2σ	4	St.d 2σ	4	St.d 2σ
SiO_2	71.79	0.54	72.11	0.67	74.49	0.35	74.70	0.42	72.39	0.31	74.72	0.38	74.28	0	74.68	0.36	74.76	0.42
TiO_2	0.37	0.18	0.26	0.03	0.11	0.08	0.05	0.05	0.25	0.07	0.08	0.05	0.11	0.04	0.18	0.14	0.14	0.11
Al_2O_3	8.06	0.20	8.25	0.26	13.89	0.21	13.77	0.14	8.00	0.06	13.87	0.03	13.81	0.11	13.80	0.18	13.97	0.24
FeO	8.10	0.07	7.95	0.07	1.33	0.24	1.38	0.24	7.97	0.18	1.32	0.14	1.54	0.03	1.29	0.14	1.44	0.26
MnO	0.38	0.08	0.29	0.11	0.10	0.01	0.03	0.03	0.24	0	0.16	0.11	0.03	0.03	0.05	0.05	0.05	0.02
MgO	0.00	0.00	0.00	0.00	0.01	0.04	0.02	0.03	0.00	0.12	0.01	0.002	0.12	0.04	0.05	0.05	0.02	0.02
CaO	0.25	0.08	0.32	0.04	0.67	0.11	0.76	0.12	0.30	0.03	0.72	0.16	0.79	0.01	0.75	0.08	0.75	0.08
Na_2O	5.95	0.17	5.82	0.12	3.58	0.21	3.48	0.07	5.60	0.09	3.56	0.10	3.76	0.03	3.54	0.15	3.31	0.10
K_2O	4.82	0.05	4.87	0.04	5.79	0.13	5.80	0.09	4.73	0.06	5.77	0.06	5.76	0.02	5.75	0.08	5.78	0.22
P_2O_5	0.09	0.09	0.00	0.00	0.00	0.00	0.00	0.00	0.05	0.03	0.00	0.00	0	0.00	0.00	0	0.00	0
P.I.	1.86	0.05	1.80	0.05	0.87	0.01	0.87	0.01	1.79	0.04	0.87	0.03	0.90	0.01	0.87	0.02	0.84	0.03
Na_2O/K_2O	1.23	0.04	1.19	0.03	0.62	0.05	0.60	0.01	1.18	0.05	0.62	003	0.65	0.03	0.63	0.03	0.57	0.04

TABLE 5. Major elements determined by SEM-EDS analyses on archaeological samples collected at Ustica.

Archaeological samples	Ust211		Ust212		Ust215		Ust220		Ust221		Ust222		Ust223		Ust224		Ust226	
Site	Lipari		Pantelleria		Lipari		Lipari		Lipari		Lipari		Pantelleria		Lipari		Lipari	
Density * g/cm^3	2.3427		2.4758		2.3505		2.3503		2.3488		2.3497		2.4532		2.3542		2.3580	
Density ** g/cm^3	2.3531		2.4185		2.3522		2.3521		2.3493		2.3555		2.4177		2.3592		2.3529	
N	5	St.d 2σ	3	St.d 2σ	4	St.d 2σ	4	St.d 2σ	3	St.d 2σ	4	St.d 2σ	5	St.d 2σ	5	St.d 2σ	5	St.d 2σ
SiO_2	74.29	0.32	71.38	0.41	74.41	0.18	74.63	0.27	74.92	0.39	74.63	0.15	71.90	0.60	74.51	0.35	74.91	0.36
TiO_2	0.06	0.06	0.23	0.05	0.07	0.03	0.10	0.04	0.01	0.02	0.19	0.12	0.24	0.11	0.10	0.10	0.15	0.10
Al_2O_3	13.83	0.19	8.16	0.06	13.96	0.07	13.78	0.17	13.86	0.27	13.88	0.25	8.11	0.15	13.76	0.13	13.90	0.07
FeO	1.41	0.09	7.63	0.28	1.39	0.09	1.40	0.10	1.31	0.11	1.54	0.14	7.71	0.40	1.42	0.09	1.38	0.19
MnO	0.08	0.06	0.40	0.13	0.08	0.05	0.05	0.05	0.08	0.06	0.00	0.01	0.34	0.21	0.15	0.07	0.06	0.04
MgO	0.03	0.07	0.00	0	0.00	0	0.00	0	0.06	0.07	0.00	0	0.00	0.01	0.03	0.06	0.00	0
CaO	0.85	0.16	0.33	0.06	0.73	0.04	0.78	0.17	0.62	0.09	0.80	0.16	0.21	0.08	0.82	0.19	0.80	0.11
Na_2O	3.62	0.14	6.32	0.18	3.74	0.20	3.49	0.13	3.47	0.24	3.34	0.15	5.95	0.20	3.34	0.25	3.45	0.10
K_2O	5.85	0.23	5.02	0.13	5.75	0.12	5.77	0.13	5.77	0.10	5.73	0.11	5.18	0.16	5.85	0.13	5.51	0.19
P_2O_5	0.00	0	0.10	0.08	0.00	0	0.00	0	0.00	0	0.00	0	0.07	0.09	0.04	0.07	0.00	0
P.I	0.89	0.03	1.94	0.02	0.89	0.02	0.87	0.02	0.86	0.04	0.84	0.03	1.90	0.07	0.86	0.03	0.84	0.06
Na_2O/K_2O	0.62	0.04	1.26	0.06	0.65	0.03	0.60	0.03	0.60	0.04	0.58	0.02	1.15	0.05	0.57	0.04	0.63	0.03

TABLE 5. Continued.

In the total alkali vs silica diagram the analysed samples plot in the field of rhyolites (Figure. 6).

Down in detail:

- *Lipari* samples have a SiO_2 ~74.2 wt%, Al_2O_3 ~ 14 wt%, Na_2O + K2O ~ 9.3 wt%, CaO ~ 0.8 wt%, FeO ~1.6 wt%. The ASI (Allumina Saturation Index, i.e. molar Al_2O_3 / CaO+Na_2O+K_2O) is ~1.03 (mean of 3 samples). Analyses of clinopyroxene microphenocrysts (30-40 μm in size, mostly subhedral to anhedral; Figure 7b) resulted in rather evolved compositions ranging from augite to hedenbergite (Figure 8). Wollastonite 36-39, Enstatite 14-16, Ferrosilite 47-51, with a (100 * Mg/Mg+Fetot) in the range 7.2 to 12.0 (Table 4).
- Palmarola samples have SiO_2 ~ 4,7 wt%, Al_2O_3 ~14 wt%, Na_2O + KvO ~9 wt%, CaO < 0.46 wt%, FeO ~1.5 wt. The ASI is ~1.12 (mean of 3 samples). Analyses of clinopyroxene microphenocrysts (~40 μm in size; Figure 7c) resulted in clynopyroxenes that are augite (Figure 7a), Wollastonite 39- 46, Enstatite 4-7, Ferrosilite 50-54, the Mg/Mg+Fetot was in the range from 21.3 to 25.1 (Table 4).
- Monte Arci samples have SiO_2 ~74.3 wt%, Al_2O_3 ~14.5 wt%, Na_2O + K_2O ~9.3 wt%, CaO ~0.8 wt%, with FeO ranging from 0.6 to 1.15 wt%. The ASI is ~1.10 (mean of 3 samples).
- Pantelleria samples have SiO_2 =72.71 wt%, Al_2Ov ~6.49 wt%, Na_2O + K_2O = 10.58 wt%, CaO ~0.28 wt%, FeO = 9.38 wt%, are strongly peralkaline (peralkalinity Index = molar (Na_2O+K_2O)/Al_2O_2 = 2.39).

6.4 PETROCHEMISTRY OF ARCHAEOLOGICAL SAMPLES

Results of microanalyses (SEM-EDS) of major elements of the archaeological obsidian samples are summarized in the Table 5. Data of silica and alkali plotted on a TAS diagram indicate that two compositional group can be distinguished (Figure 9).

- Group A samples have SiO_2 ~71.9 wt%, Al_2O_2 ~ 8.1 wt%, Na_2O + K2O ~ 10.8 wt%, CaO ~ 0.3 wt%, FeO ~ 7.9 wt%; they are peralkaline with a Peralkalinity Index ~ 1.9 (mean of 5 samples).
- Group B samples have SiO_2 ~74.6 wt%, Al_2O_3

Archaeological samples	UST. 211	UST. 211	UST. 220	UST. 220	UST. 221	UST. 224	UST. 224	UST. 226	UST. 226
SiO_2	49.04	46.25	45.07	46.06	49.22	44.61	45.54	48.55	45.81
TiO_2	0.00	0.07	0.00	0.00	0.47	0.24	0.06	0.29	0.51
Al_2O_3	3.77	2.54	7.92	5.10	4.97	7.13	8.39	0.84	3.53
FeO	25.38	28.65	25.55	25.04	25.08	24.52	22.87	27.97	26.98
MnO	1.51	2.00	1.13	1.71	1.52	1.09	1.12	2.85	1.87
MgO	1.89	1.12	0.39	1.31	1.53	1.53	1.03	2.51	2.56
CaO	16.02	18.70	18.97	20.05	14.87	19.61	19.79	16.69	18.73
Na_2O	1.28	0.85	1.03	0.73	1.43	1.16	1.11	0.46	0.83
K_2O	0.62	0.16	0.15	0.15	0.57	0.21	0.14	0.04	0.02
Cr_2O_3	0.00	0.00	0.09	0.00	0.00			0.02	0.00
Tot.	99.50	100.35	100.24	100.11	99.57	100.10	100.05	100.22	100.74
Wo	41.66	43.86	48.09	48.41	40.66	47.97	50.65	39.72	43.20
En	6.82	3.66	1.38	4.40	5.83	5.21	3.67	8.32	8.21
Fs	51.51	52.47	50.54	47.19	53.51	46.82	45.68	51.96	48.58
Mg/Mg+Fe * 100	11.70	6.52	2.65	8.53	9.83	10.01	7.43	13.81	14.46

TABLE 6. Major elements determined by SEM-EDS analyses on clinopyroxene microphenocrysts observable in the archaeological samples of Ustica.

Specimen	Density g/cm^3 * Experimental	Density g/cm^3 ** Calculated	H_2O (wt%) Rim	H_2O (wt%) Core
UST-180	2.47	2.43	0.27	0.12
UST-186	2.45	2.42	0.23	0.16
UST-191	2.35	2.35	0.20	0.29
UST-192	2.34	2.35	0.21	0.10
UST-195	2.47	2.42	0.28	0.19
UST-201	2.34	2.35	0.2	0.27
UST-203	2.33	2.36	-	-
UST-206	2.35	2.35	0.24	0.12
UST-208	2.36	2.35	0.14	0.15
UST-211	2.34	2.35	0.26	0.13
UST-212	2.48	2.42	0.14	0.16
UST-215	2.35	2.35	0.81	0.88
UST-220	2.35	2.35	0.13	0.14
UST.221	2.35	2.35	0.91	0.62
UST-222	2.35	2.36	0.52	0.62
UST-223	2.45	2.42	0.13	0.07
UST-224	2.35	2.35	0.31	0.13
UST-226	2.36	2.35	0.3	0.20

TABLE 7. Hydration gradient measured in our archaeological samples by means of FT-IR analyses. * density measurements with a high-precision analytical balance. ** density calculated according to Ochs and Lange [1999].

~ 13.9 wt%, Na_2O + K2O ~ 9.3 wt%, CaO ~ 0.76 wt%, FeO ~ 1.4 wt%; they have a P.I. < 1. The ASI is ~ 1.04 (mean of 13 samples). Analyses of clinopyroxene microphenocrysts (~40 μm in size) resulted in rather evolved clynopyroxenes ranging from augite to hedenbergite, Wollastonite $_{26 - 51}$, Enstatite $_{1 - 12}$, Ferrosilite $_{46 - 68}$, with a (100* Mg/Mg+Fetot) in the range 2.7 to 18.9 (Table 6, Figure 1).

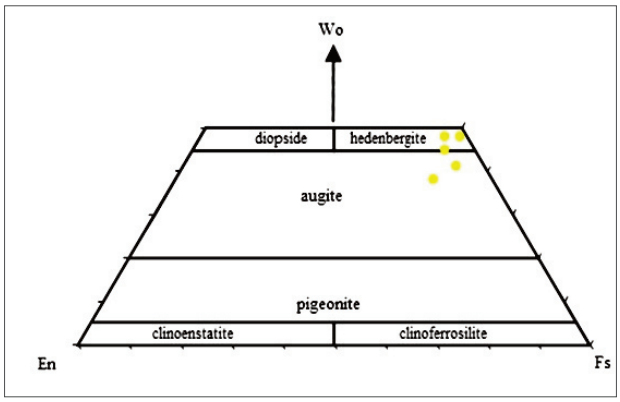

FIGURE 10. Composition of pyroxenes of the archaeological samples [Morimoto et al., 1989].

6.5 H_2O CONTENT

Water concentrations were derived from total H_2O absorption band (3550 cm^{-1}) using a straight baseline correction and applying the Beer-Lambert equation, $c = (MW\ A)/(d\ \rho\ \varepsilon)$, where **c** is the wt.% of dissolved H2O, MW the molecular weight of H_2O, A the height of the absorption peak, **d** the sample thickness in cm, **ρ** the glass density in g L^{-1}, **ε** the molar extinction coefficient. The adopted molar extinction coefficient (ε^{3550}) was 84 L mol^{-1} cm^{-1} [Zhang et al., 1997]. The glass density **ρ** was obtained according to Ochs and Lange [1999], being the difference with the experimental density negligible (Table 7).

H_2O content was determined by FT-IR spectroscopy both on rims and cores of all the archaeological samples. We report in Table 6 for each archaeological obsidian flake analyzed, H_2O concentration (rim and core) and density (experimental and calculated).

The measured densities of obsidians of the Group A (~2.42 g cm^{-3}) are greater than those of glasses of the Group B (~2.35 g cm^{-3}).

The dissolved H_2O ranges from 0.13 to 0.91 wt% in the rim of the samples, and from 0.07 to 0.88 wt% in the core of the samples.

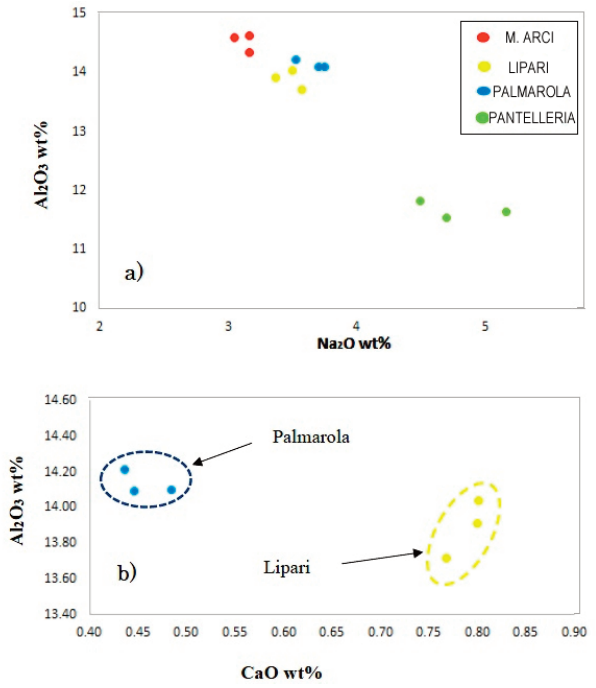

FIGURE 11. Discriminating obsidian sources with major elements binary diagrams. a) Na_2O vs Al_2O_3: M.Arci obsidians have higher values of Al_2O_3 and lower of Na_2O than the other sources; but Lipari an Palmarola tend to overlap. b) CaO vs Al_2O_3: Palmarola obsidian have lower values of CaO respect to Lipari.

7. DISCUSSION

7.1 PETROCHEMICAL DATA

Pantelleria obsidians clearly differ from all the other pery-Tyrrhenian sources by the lowest content in SiO_2, the highest content in alkali, high content FeO and their characteristic peralkalinity. Their chemical signature is thus the most easily reconizable among all the others. Less clear is the distiction among the other three sources with Lipari obsidians being in an intermediate position between Palmarola and Monte Arci for many chemical variables. However Lipari obsidians are separated from Palmarola and Monte Arci by their Ca, Na, Al content. In a diagram Na_2O vs Al_2O_3 Monte Arci samples are higher in Al_2O_3 (~15 wt%) and lower in Na_2O (~ 3wt%), (Figure 11a). Nevertheless, the most striking distinguishing features is the occurence of biotite microphenocrysts. In a diagram CaO vs Al_2O_3 diagram Palmarola samples are lower in CaO (< 0.5%) compared to Lipari samples (>0.8%) (Figure 11b).

On the basis of the silica and alkali composition, we confirm that the archaeological obsidian flakes tend to gather in two main groups (Figure 9b). We can assign to the Group A a provenance from Pantelleria source for a slightly lower silica content and a significantly higher content of total alkali. The CaO content (>0.8%) suggests that the Group B probably belong to Lipari.

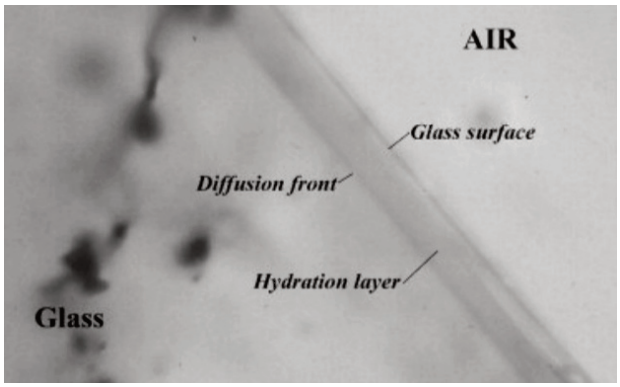

FIGURE 12. Hydration rim (or layer) on an obsidian sample by optical microscope. After Stevenson [2011].

7.2 Mineral assemblages and mineral chemistry

A comparison between the analysis carried out on the pyroxenes and the literature data [Acquafredda and Paglionico, 2004] allows to conclude that the pyroxene compositions distinguish Palmarola (En mol % = 13- 20 and 100* Mg/Mg+Fe= 21 -25) from Lipari sources (En mol % = 4-8 % 100* Mg/Mg+Fe = 7-12).

The analysis carried out in the pyroxenes of the archaeological samples allows to conclude that the Group B present pyroxene compositions corresponding to the Lipari source. Therefore, we can assign to the Group B a provenance from the Lipari source. Nevertheless, in our set two samples (UST-201 and UST- 208) remain somehow enigmatic since for the enstatite content (respectively 10.95% and 11.68%) and ratio Mg/Mg+Fe (respectively 18.48 and 18.87) in clinopyroxene, distinctly higher than Lipari samples and lower with respect to the Palmarola samples.

7.3 H_2O CONTENT

The H_2O analysis allows to detect a hydration gradient that can give a rough evaluation of the obsidian tool's age since the time of its chipping, applying the empirical equation proposed by Friedman and Smith [1960]. About fifty years ago Friedman and Smith recognized the obsidian hydration phenomenon and proposed an empirical dating method based on the conversion of the optically measured hydration depth to an absolute age [Liritzis and Laskaris, 2011], (Figure 12).

Our FT-IR results show a compositional gradient of H2O content in the range of 0.3 to 0.1 wt% from the rim to the core of 10 obsidians flakes (Table 6); but de-

spite that we have not clearly identified any hydration rim in our samples.

7. CONCLUSIONS

A multi-disciplinary analytical study allowed us to characterize a group of archaeological obsidian collected in the island of Ustica, also by comparison with geological obsidian samples of the four Central-Mediterranean outcrops exploited during the prehistory: M. Arci, Palmarola, Lipari and Pantelleria.

With regard to provenance, out of 18 samples examined, 5 (27%) are attributable to the obsidian outcrops of Pantelleria, and 13 (73%) to the island of Lipari. The attribution of 5 samples to Pantelleria has appeared evident starting from the physical analysis: green colour in transmitted light, and higher density (2.45-2.47 g cm^{-3}) compared to that of obsidians from M. Arci, Lipari and Pantelleria (2.35-2.37).

SEM-EDS analysis of the major elements performed on glass bulk of archaeological samples, while confirming the Pantelleria provenances characterized by a P.I. >1, permitted to distinguish three other sources, thanks to discriminating diagrams Na_2O vs Al_2O_3 and CaO vs Al_2O_3.

Effective discrimination between the main sources of obsidian is achievable also by SEM-EDS microanalysis of the crystals present in the vitreous mass: e.g. the compositions of some pyroxenes (namely, the amount of enstatite component) distinguish Palmarola source from Lipari.

At last, we have developed a preliminary study on the H_2O content of our obsidian fragments, in order to verify if there is a hydration gradient between the edge and the core of the sample, caused by the absorption of atmospheric water in the worked edges. This check is useful to select the samples on which to carry out a search for the hydration rim or layer, whose thickness would allow an approximate calculation of the age of the tool.

REFERENCES

Acquafredda P., Andriani T., S. Lorenzoni S., Zanettin E. (1999) Chemical Characterization of Obsidians from Different Mediterranean Sources by Non-destructive SEM-EDS Analytical Method. Journal of Archaelogical Science 26. 315-325

Acquafredda P. and Paglionico A. (2004) SEM-EDS microanalysis of microphenocrysts of Mediterranean obsidians: a preliminary approach to source discrimination. Eur. J. Mineral. 16, 419-429.

Barberi, F., Borsi, S., Ferrara, G. & Innocenti, F. (1967) Contributo alla conoscenza vulcanologica e magmatologica delle isole dell'arcipelago Pontino. Memorie della Societa` Geologica Italiana 17, 581-606.

Bellot-Gurlet, L., Poupeau, G., Dorighel, O., Calligaro, T., Dran, J. C., & Salomon, J. (1999). A PIXE/fission-track dating approach to sourcing studies of obsidian artefacts in Colombia and Ecuador. Journal of Archaeological Science, 26(8), 855-860.

Bigazzi, G., Bonadonna, F.P., Belluomini, G., Malpieri, L. (1971) Studi sulle ossidiane italiane. IV. Datazione con il metodo delle tracce di fissione. Boll. Soc. Geol. It., 90, 469-480.

Bigazzi G., Oddone M., Radi G. (2005) The Italian obsidian sources. Archeometriai Mùhely 2005/1.

Civetta, L., Cornette, Y., Gillot, P.Y., Orsi, G. (1988) The eruptive history of Pantelleria (Sicily Channel). Bull. Volcan., 50, 47-57.

De Francesco, A. M., and Crisci, G. M. (1999) Provenienza delle ossidiane dei siti archeologici di Pianosa (ArcipelagoToscano) e Lumaca (Corsica) con il metodo non distruttivo in Fluorescenza X, in Il primo popolamento Olocenico dell'area corso-toscana (eds. C. Tozzi and M. C. Weiss), 253-8, Edizioni ETS, Pisa.

De Francesco, A. M., and Crisci, G. M. (2003) L'ossidiana, in Tozzi, C., Zamagni, B., Gli scavi nel villaggio neolitico di Catignano (1971-1980), in Origines, studi e materiali pubblicati a cura dell'Istituto Italiano di Preistoria eProtostoria, 239-40, Firenze.

De Francesco, A. M., Bocci, M., and Crisci, G. M. (2004) Provenienza dal Monte Arci per le ossidiane di alcuni siti archeologi dell'Italia Centrale e della Francia Meridionale, in Proceedings of 2° Convegno Internazionale 'L'ossidiana del Monte Arci nel Mediterraneo', Pau (Cagliari), 28-30 novembre 2003, 303-9, Ed. AV (CA).

De Rita, D., Funiciello, R., Pantosti, A., Velonà, M. (1989) Caratteristiche geologico-strutturali delle Isole Pontine nordoccidentali. Atti Convegno "Incontro con la Geologia Circeo, Sabaudia 1984", 43-64.

de Vita S., Guzzetta G., Orsi G. (1995) Deformational

features of the Ustica volcanic Island in the Sothern Tyrrhenian Sea Italy. Terra Nova 7. 623-6329

de Vita S., Laurenzi M.A.,Orsi G., Voltaggio M. (1998) Application of 40Ar/39Ar and 230Th dating methods to the chronostratigraphy of quaternary basaltic volcanic area: the Ustica Island case history. Quaternary Int 4 (48).117-127.

Donato P., Barba L., De Rosa R., Niceforo G., Pastrana A., Donato S., Lanzafame G., Mancini L., Crisci G.M. (2017) Green, grey and black: A comparative study of Sierra de las Navajas (Mexico) and Lipari (Italy) obsidians. Quaternary International, 467,369-390.

Foresta Martin F., Di Piazza A., Doriano C., Carapezza M.L., Rotolo S.G., Sagnotti L. (2017) New insights on the provenance of obsidian fragments of Ustica Island (Palermo, Sicily). Archaeometry, 59(3), 435-454.

Foresta Martin F. and La Monica M. (2018) The Black Gold that came from the sea. A review of obsidian studies at the island of Ustica, Italy. Annals of Geophysics, 61. Doi: 10.4401/ag-7686.

Forni, F., Lucchi, F., Peccerillo, A., Tranne, C. A., Rossi, P. L. and Frezzotti, M. L. (2013) Stratigraphy and geological evolution of the Lipari volcanic complex (central Aeolian archipelago). Geological Society, London, Memoirs, 37(1), 213-279.

Francaviglia V. (1984) Characterization of Mediterranean obsidian sources by classical petrochemical methods. Preistoria Alpina - Museo Tridentino di Scienze Naturali, Vol. 20. 311-332.

Freund, K.P., Tykot, R.H., Vianello, A. 2017 Contextualizing the role of obsidian in Chalcolithic Sicily (c.3500-2500 BC). Lithic Technol. 42, 35e48.

Friedman, I. and Smith, R. L. (1960). Part I, The Development of the Method. American Antiquity, 25(4), 476-493.

Le Bas M.J. , Le Maitre R.W. , Streckeisen A., Zanettin B. (1986). A Chemical Classification of Volcanic Rocks Based on the Total Alkali-Silica Diagram Journal Petrol. 27(3), 745-750.

Liritzis, I. and Laskaris, N. (2011) Fifty years of obsidian hydration dating in archaeology. Journal of Non-Crystalline Solids, 357(10).

Macdonald, R. (1974) Nomenclature and petrochemistry of the peralkaline oversaturated extrusive rocks. Bulletin volcanologique, 38(2), 498-516.

Montanini, A. (1992) Il complesso vulcanico di Monte Arci (Sardegna): aspetti petrologici e geochimici. Ph. D. thesis, Università di Modena.

Montanini, A. & Villa, J.M. (1993) 40Ar/39Ar chronostratigraphy of Monte Arci volcanic complex (Western Sardinia, Italy). Acta Volcan., 3, 229-233.

Montanini, A., Barbieri, M., Castorina, F. (1994) The role of fractional crystallization, crustal melting and magma mixing in the petrogenesis of rhyolites and mafic inclusion-bearing dacites from the Monte Arci volcanic complex (Sardinia, Italy). J. Volcan. Geoth. Research, 61. (95-120).

Morimoto N., Fabries J., Ferguson A.K., Ginzburg I.V., Ross M., Seirfert F.A. & Zussman J. (1988) Nomenclature of pyroxenes. Mineral. Mag. 52, 535-550.

Ochs, F. A. and Lange, R. A. (1999) The density of hydrous magmatic liquids. Science, 283(5406), 1314-1317.

Rotolo S.G., Scaillet S.,La Felice S., Vita Scaillet G. (2013) A revision of the structure and stratigraphy of pre-Tufo Verde ignimbrites at Pantelleria (Strait of Sicily). Journal of Volcanology and Geothermal Research, 250(61-74).

Skinner, C. E.and Moratto, M. J. (1995) Obsidian Hydration Studies. Archaeological Investigations, PGT-PG&E Pipeline Expansion Project, Idaho, Washington, Oregon, and California, 5, 5.

Stevenson, C. M. and Novak, S. W. (2011) Obsidian hydration dating by infrared spectroscopy: method and calibration. Journal of Archaeological Science, 38(7), 1716-1726.

Tykot, R.H. (1996) Obsidian Procurement and Distribution in the Central and Western Mediterranean. J. Mediterranean Archaeol., 9, 39-82.

Tykot R.H., Setzer T., Glascock M.D., Speakman R.J. (2005) Identification and Characterization of the Obsidian Sources of the Island of Palmarola, Italy, Geoarchaeol. Bioarchaeol. Stud. 3, 107-111.

Williams - Thorpe O. (1995) Obsidian in the Mediterranean and the near east: a provenancing story. Archaeometry. 37,2. (217-248)

Zanchetta, G., Sulpizio, R., Roberts, N., Cioni, R., Eastwood, W.J., Siani, G., Caron, B., Paterne, M., Santacroce, R., (2011) Tephrostratigraphy, chronology and climatic events of the Mediterranean basin during the Holocene: an overview. Holocene 21, 33e52.

Zhang Y, Belcher R, Ihinger PD, Wang L, Xu Z, Newman S (1997). New calibration of infrared measurement of water in rhyolitic glasses. Geochimica Cosmochimica Acta 61 3089-3100

CORRESPONDING AUTHOR: Franco FORESTA MARTIN ,
Laboratorio Museo di Scienze della Terra Isola di Ustica,
Palermo, Italy
email: sidereus@rocketmail.com

© 2019 the Istituto Nazionale di Geofisica e Vulcanologia.
All rights reserved